Study of van Gieson's picrofuchsin staining on second-harmonic generation in type I collagen

Hanping Liu (刘汉平)[1], Zhengfei Zhuang (庄正飞)[1], Lingling Zhao (赵羚玲)[2], Junle Qu (屈军乐)[2], and Xiaoyuan Deng (邓小元)[1]

[1]*School for Information and Optoelectronic Science and Engineering, South China Normal University, Guangzhou 510700*

[2]*Key Laboratory of Optoelectronic Devices and Systems (Ministry of Education and Guangdong Province), Institute of Optoelectronics, Shenzhen University, Shenzhen 518060*

Received June 23, 2008

Second-harmonic generation (SHG) microscopy is a recently developed nonlinear optical imaging modality for imaging tissue structures with submicron resolution and is a potent tool for visualizing pathological effects of diseases. In this letter, we present our investigation on the influence of van Gieson's (VG) alcoholic picrofuchsin staining on SHG in type I collagen (from tendon-rich C57BL/6). Multi-channel imaging and spectra analysis show that the strong SHG signal produced in fresh collagen type I fiber has been greatly suppressed after VG staining, which indicates that staining may induce the structural or characteristic changes of SHG-dependent crystal formed by collagen constituents, such as glycine, proline, and hydroxyproline.

OCIS codes: 180.4315, 190.4160, 170.6930.

doi: 10.3788/COL20080612.0882.

Second harmonic generation (SHG) is the 2nd-order optical nonlinear process related to second nonlinear susceptibility $\chi^{(2)}$ of the material and the electric field vector E of light[1]: $P_{\rm SHG} = \chi^{(2)} \otimes E \otimes E$, $\chi^{(2)} = N_s\langle\beta\rangle$, where $\otimes$ represents a combined tensor product and integral over frequencies and $P_{\rm SHG}$ is the induced polarization vector. $\chi^{(2)}$ is introduced by orientational average of molecular hyperpolarizability β of molecules, which shows the need for a non-centrosysmetrical environment of SHG, and N_s is the molecule density. SHG is a coherent process in which two near-infrared incident photons at the fundamental frequency are converted into a single photon at twice the frequency by scattering[2]. Like two-photon excitation fluorescence (TPEF), SHG is also a "nonlinear" process, whose occurrence depends nonlinearly (quadratic dependence) on the excitation intensity. Such intensity-squared dependence forms the basis of the high-resolution nonlinear optical sectioning scheme: out-of-focus excitation rarely happens, thus out-of-focus photobleaching and phototoxicity are greatly reduced[2]. However, unlike the absorption process of TPEF, SHG has its own unique features. SHG does not involve the excited state, thus it conserves the energy and preserves the coherence of light. SHG microscopy which takes the advantage of SHG phenomenon for microscopic imaging has thus been developed to be a valuable tool for non-invasive biological specimen imaging with submicron resolution[3−7].

Collagen fiber becomes the focus of the SHG microscopic imaging studies because of its special characteristic. Collagen molecules are naturally organized into structures on the scale of light wavelength, lack a center of inversion symmetry, and have the first hyperpolarizabilities large enough for SHG[8−11]. Collagen is the most abundant structural protein in the body. Based on their different supramolecular organization patterns, collagens are generally categorized as fibrillar or nonfibrillar[12]. Type I collagen is the predominant form of fibrillar collagen and one of the major constituents of tissues. The first study related to SHG in biological tissues was reported in 1971[8]. Since then, a series of exhaustive studies of the harmonic signal in type I collagen of a rat-tail tendon was conducted by investigators[12−16]. Since SHG is coherent, specimen information can be derived from the directionality of the SHG emission. SHG signal has been proved useful for differentiating immature and mature fibrillar collagens. In an experiment of 10-day-old rat tail tendon, it was found that immature fibril segments scatter SHG backward, whereas mature fibrils scatter SHG forward[2].

The characteristic changes in the organization of fibrillar collagen are known to be highly related to the pathological processes and diseases, such as cancer, aging, and wound healing[17,18]. Collagen fiber thus could potentially serve as an early diagnostic marker of diseases. As a result, the derangements of collagen structure and function play a pivotal role for the understanding of pathophysiological conditions. SHG produced from collagen has been addressed as a new approach for analyzing the molecular architecture of collagen[12].

Unfortunately, collagen SHG is extremely sensitive to the biochemical properties of the solution in which the fibrils reside. To extend its applications in biomedicine, it is necessary to take a further look at those factors which may affect the generation of the second harmonic signal. Factors such as fibril diameter, pH value, and osmotic stress on collagen SHG have been studied. It is found that the ion density of the solution significantly affects the ratio of forward to backward signals (F/B) in SHG microscopy. The magnitude of F/B can be ten folds lower under high-salt conditions. Based on this experimental result and other experimental conditions, Williams *et al.* inferred that the decrease of F/B with ionic strength is possibly due to a sub-resolution struc-

tural change in collagen fiber[15].

Van-Gieson's (VG) picrofuchsin staining is the most common histological staining method for collagen fiber processing on pathological evaluation. VG picrofuchsin is a type of dye mixture solution mainly including acid fuchsin (AcF) and picric acid (PA)[19]. It is expected that the staining process may cause some changes in physical and/or biochemical characteristics, but it remains unknown that in which way such changes occur and how such changes affect (increase or reduce) the generation of second-harmonic signals in collagen fiber. The investigation of the influence of staining process on the SHG signal will provide us certain types of clues on the basic structure of collagen fiber and the mechanism of dyes acting on collagen fiber, as SHG signal is an indicator of the physical and/or biochemical features in collagen fiber.

The imaging and spectrum system implemented in this letter (as shown in Fig. 1) mainly consists of a coherent Mira 900-F mode-locked femtosecond Ti:sapphire laser source (120-fs pulse width, 76-MHz repetition rate, and $700-980$ nm tunable wavelength) and a confocal laser scanning microscope (TCS SP2, Leica, Germany), which is used to realize three-dimensional (3D) high-resolution imaging. The near-infrared excitation light is reflected by the dichroic beam-splitter (DBS) and focused onto the specimen by the objective. The emitted SHG and the fluorescence signals from the specimen are collected by the same objective and pass through the DBS and then are dispersed by the prism spectrometer before being detected by photomultiplier tubes (PMTs). Oil-immersion objective with the numerical aperture (NA) of 1.35 (Plan-Apochromat 63×, Zeiss, Germany) is used for microscopic imaging. By scanning the slit of the prism spectrometer inside the scanning head of the confocal system, the spectra of the specimen can be obtained.

Our experimental materials, type I collagen fiber, are from the C57BL/6 mice-tails. The tails were collected and kept in −80 °C refrigerator ready for slicing. All mice manipulations were done in accordance with policies of the Institute Animal Care and Use Committee. Tails were then taken out from the −80 °C refrigerator and put in −18 °C refrigerator for 6 h before being sliced. Each tail was cut sequentially parallel to collagen fiber by a cryostat (CM1850, Leica, Germany) with the slice-thickness of 10 μm. Slices were randomly sampled to two groups: fresh frozen group and staining group. Frozen slices were conserved in the liquid nitrogen immediately after slicing. Our experimental samples of staining collagen were elaborately prepared as follows. Firstly, the whole slice was fixed in 95% alcohol for half a minute. Then, only part of the slice along the axis of collagen fiber was stained by VG staining for 3 min, and the rest part remained unstained for comparison. In our experiment, such experimental design was expected to strictly control the factors that may affect the SHG signals due to different experimental conditions to the lowest extent. For example, such design avoids the possible influence of different density distribution of collagen fiber on different slices and the possible influence of different alignment direction of different collagen fibers relative to the polarization of excitation laser light. Figure 2 shows the image taken according to our experimental scheme. The image is formed by Nikon TS100 (Japan) and the objective is Nikon E Plan 40X/0.10 (Japan). A clear interface between the left side (VG stained) and the right side (fixed by 95% alcohol only) can be seen.

Figure 3 shows the images of SHG, TPEF, and the combined image of SHG and TPEF of the stained collagen fiber, in which the left side is VG stained area and the right one is non-stained area but fixed by 95% alcohol. The SHG signals were collected from 400 to 430 nm (green, pseudo-color) (Fig. 3(a)) and the TPEF signals were from 550 to 700 nm (red, pseudo-color). All the data were obtained at the excitation wavelength of 830 nm and the light power on the sample was less than 15 mW. Figures 3(a) and (b) show that there is weak TPEF but strong SHG signal on the non-stained area. However, the result is the opposite on the stained area, i.e., there is strong TPEF but weak SHG signal. This phenomenon

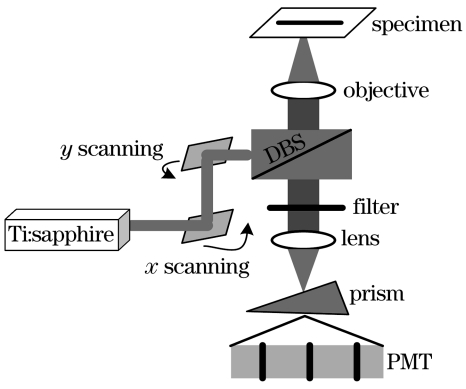

Fig. 1. Schematic diagram of imaging and spectrum analysis system.

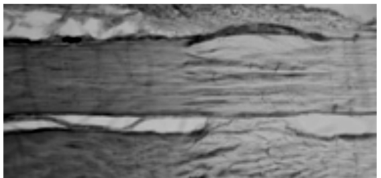

Fig. 2. Image of collagen fiber partly stained by VG picrofuchsin (left) and partly fixed by 95% alcohol (right).

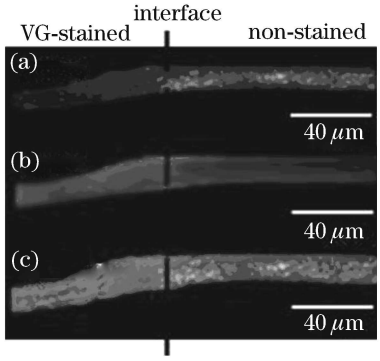

Fig. 3. Images of (a) SHG, (b) TPEF, and (c) combined image of SHG and TPEF of partly stained collagen fiber by VG picrofuschin (left) and fixed by 95% alcohol only (right).

can be demonstrated more clearly in the combined image of SHG and TPEF in Fig. 3(c), which shows that there is strong SHG in non-stained area, while in the VG-stained area, TPEF is dominant. Figure 3 also shows an interface that distinguishes VG stained and non-VG stained areas as shown in Fig. 2. In order to further investigate the difference between VG stained and non-stained areas, particularly those near the interface, the magnified images of the areas near the interface are shown in Fig. 4. It is shown that there is no clear interface between VG stained and non-stained areas. Instead, there is a transition area in which SHG and TPEF signals coexist. The formation of this transition area is possibly due to the migration of the dye molecules from the VG stained area to the non-stained area. Figure 4(d) shows the corresponding spectra from VG stained area to the transition area and to the non-VG stained area in the combined image of SHG + TPEF in Fig. 4(c). According to the spectral features of SHG and fluorescence, the sharp peak represents SHG and the broad one is fluorescence, which demonstrates that in VG stained area, SHG is not resolvable but TPEF is strong; in the transition area, both the SHG and TPEF signals are observable; however, in the non-VG stained area, SHG is strong, but TPEF cannot be detected.

For comparison, SHG and TPEF images of fresh frozen type I collagen fiber are shown in Fig. 5, which shows that in the fresh frozen collagen fiber, SHG is very strong (Fig. 5(a)). On the other hand, TPEF signals are virtually un-detectable (image is not shown here). Figure 5(b) shows the combined image of SHG and TPEF, which has negligible difference from SHG image, indicating that TPEF has no contribution to the image. The spectra experimental results in Fig. 5(c) clearly show that there are

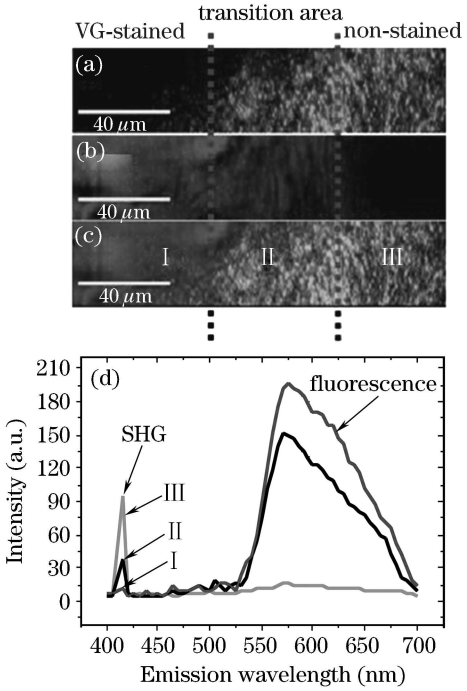

Fig. 4. Magnified images of (a) SHG, (b) TPEF, and (c) combined image of SHG and TPEF (c) around the interface of VG stained and non-VG-stained area. (d) The corresponding spectra of the specimen from 400 to 700 nm in areas I, II, and III in (c).

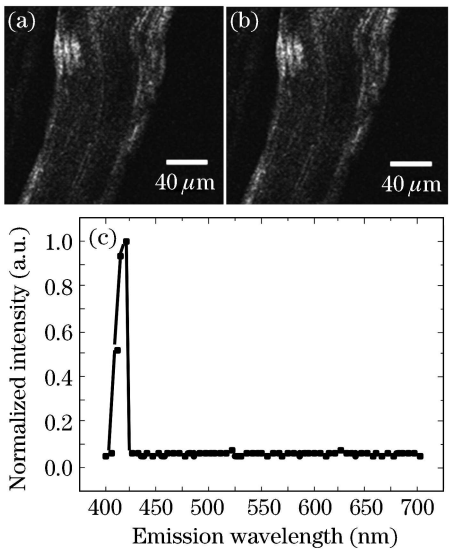

Fig. 5. (a) Image of SHG, (b) combined image of SHG and TPEF, and (c) the corresponding spectra from 400 to 700 nm in fresh frozen collagen fiber.

strong SHG but no TPEF signals. It is reasonable now to conclude that staining has an obvious suppression effect on SHG in collagen type I.

Abundant in tendon-rich tissue such as rat tails, the fibrous type I collagen has the fundamental structure unit of protein of 300-nm length and 1.5-nm diameter that consists of three left-handed coiled subunits: two α1(I) chains and one α2(I). Each chain contains precisely 1050 amino acids. These amino acids make up the characteristic repeating motif glycine (Gly)-X-Y, where X and Y are generally proline (Pro) and hydroxyproline (Hyp), respectively. Three chains wind around one another into a characteristic right-handed triple helix[20]. Each amino acid has a precise function. The side chain of glycine, a hydrogen atom, is the only one that can fit into the crowded center of a three-stranded helix. Hydrogen bonds linking the peptide bond NH of a glycine residue with a peptide carbonyl (C=O) group in an adjacent polypeptide help hold the three chains together. The fixed angle of the C–N peptidyl-proline or peptidyl-hydroxyproline bond enables each polypeptide chain to fold into a helix with a geometry such that three polypeptide chains can twist together to form a three-stranded helix. Many three-stranded type I collagen molecules then pack together side-by-side forming microfibrils with a diameter of $50-200$ nm. In microfibrils, adjacent collagen molecules are displaced from one another by 67 nm, about one-quarter of their length. It is sure that microfibrils grow layer by layer to form fibrils, but how the microfibrils are laterally packed together in the most efficient way is not solved. Three possible packing models from microfibril into fibril are assumed to be hexagonal, cylindrical, and spiral, respectively. The very recent study shows that the packing topology of collagen molecules is such that packing neighbors are arranged to form a supertwisted (discontinuous) right-handed microfibril that interdigitates with neighboring microfibrils. This interdigitation establishes the crystallographic superlattice, which is formed of quasihexagonally packed collagen molecule[21]. Both glycine and hydroxyproline,

two major constituents of collagen fibrils, generate second harmonic in crystal form[15].

VG staining is designed to differentiate between collagen fiber and muscle fiber. The principle underlying the VG staining for collagen fiber is very complex and not very clear yet, but the widely accepted explanation of the mechanism is that it is the combination of physical properties of the tissue and chemical bonding[19]. The physical properties such as the steric hindrance come into effect whenever two denatured protein chains closely appose or cross-link to each other. The dominant chemical bonding of dye to VG picrofuchsin is believed to be hydrogen bonds. Due to the parallel, uniform fiber organization of collagen, the majority of peptide groups, and hydroxyl-bearing amino acid residues may be available for hydrogen bond formation to dyes. However, in the triple-helix conformation, glycine is the most dominant residue in collagen because it occupies every third residue.

Multi-channel imaging and spectra analysis show that the strong SHG signals produced in fresh collagen fiber has been greatly suppressed in VG stained collagen fiber, indicating that if hydrogen bonds do form between VG picrofuchin and the collagen fiber, they induce the breach of the characteristic of collagen fiber, and such damage possibly occurs on glycine, the predominant residues that make up the collagen in a crystal form along with other constituents like praline and hydroxyproline, thus strongly affect the generation of second-harmonic in collagen type I. The appearance of the strong fluorescence signals after VG-staining possibly is because of the dye of acid fuchsin, which has fluorescence emission at about 630 nm under the 540-nm single photon excitation. Fresh type I collagen from tendon-rich rat-tail in our experiments has almost no fluorescence, which is consistent with other researchers' conclusion, i.e., although tendon collagen shows virtually no fluorescence, dermal collagen shows quite a significant amount, which may relate to the amount of collagen glycosylation and cross-linking[15].

The authors gratefully thank the National Natural Science Foundation of China (No. 30470495) and the Institute of Optoelectronics, Shenzhen University for their support and the authors also thank Ms. Danni Chen for her helpful assistances. X. Deng is the author to whom the correspondence should be addressed, her e-mail address is xiaoyuandeng@yahoo.com.cn.

References

1. P. J. Campagnola and L. M. Loew, Nature Biotechnol. **21,** 1356 (2003).
2. W. R. Zipfel, R. M. Williams, and W. W. Webb, Nature Biotechnol. **21,** 1369 (2003).
3. P. J. Campagnola, A. C. Millard, M. Terasaki, P. E. Hoppe, C. J. Malone, and W. A. Mohler, Biophys. J. **81,** 493 (2002).
4. A. Zoumi, A. Yeh, and B. J. Thromberg, PNAS **99,** 11014 (2002).
5. X. Deng, E. D. Williams, E. W. Thompson, X. Gan, and M. Gu, Scanning **24,** 175 (2002).
6. D. A. Dombeck, K. A. Kasischke, H. D. Vishwasrao, M. Ingelsson, B. T. Hyman, and W. W. Webb, PNAS **100,** 7081 (2003).
7. X. Deng, X. Wang, H. Liu, Z. Zhuang, and Z. Guo, J. Biomed. Opt. **11,** 024013 (2006).
8. S. Fine and W. P. Hansen, Appl. Opt. **10,** 2350 (1971).
9. I. Freund and M. Deutsch, Opt. Lett. **11,** 94 (1986).
10. B. Li, Z. Zhang, and S. Xie, Chin. Opt. Lett. **4,** 348 (2006).
11. J. Chen, S. Zhuo, T. Luo and J. Zhao, Chin. Opt. Lett. **4,** 598 (2006).
12. P. Stoller, K. M. Reiser, P. M. Celliers, and A. M. Rubenchik, Biophys. J. **82,** 3330 (2002).
13. S. Roth and I. Freund, J. Chem. Phys. **70,** 1637 (1979).
14. T. Yasui, Y. Tohno, and T. Araki, J. Biomed. Opt. **9,** 259 (2004).
15. R. M. Williams, W. R. Zipfel, and W. W. Webb, Biophys. J. **88,** 1377 (2005).
16. A. Erikson, J. Örtegren, T. Hompland, C. de Large Davies, and T. Lindgren, J. Biomed. Opt. **12,** 044002 (2007).
17. P. A. Netti, D. A. Berk, M. A. Swartz, A. J. Grodzinsky, and R. K. Jain, Cancer Res. **60,** 2497 (2000).
18. E. Brown, T. McKee, E. diTomaso, A. Pluen, B. Seed, Y. Boucher, and R. K. Jain, Nature Med. **9,** 796 (2003).
19. P. Prentø, Histochem. **99,** 163 (1993).
20. R. Berisio, L. Vitagliano, L. Mazzarella, and A. Zagari, Protein Sci. **11,** 262 (2002).
21. J. P. R. O. Orgel, T. C. Irving, A. Miller, and T. J. Wess, PNAS **103,** 9001 (2006).